JPEDAV (2005) 26:547-554
DOI: 10.1361/154770305X66709
1547-7037/$19.00 ©ASM International

Self-Diffusion and Impurity Diffusion in Silicon Dioxide

Masashi Uematsu

(Submitted July 19, 2005)

We present experimental and simulation results of silicon (Si) self-diffusion and boron (B) diffusion in silicon dioxide (SiO_2), and examine the effect of nitrogen (N) on diffusion in SiO_2. To elucidate the point defect that mainly governs the diffusion in SiO_2, the diffusion of implanted ^{30}Si in thermally grown $^{28}SiO_2$ is investigated. The experimental results show that Si self-diffusivity increases with decreasing distance between the ^{30}Si and Si-SiO_2 interface. We propose a model in which SiO molecules generated at the interface and diffusing into SiO_2 enhance Si self-diffusion, and the simulation results fit the experimental results. The B diffusivity also increases with decreasing the distance, which indicates that B diffusion is enhanced by SiO. In addition, we investigate the effects of B and N on SiO diffusion in SiO_2. We show that the existence of B increases SiO diffusivity and hence decreases the viscosity of SiO_2. On the other hand, the incorporation of N decreases SiO diffusivity, which reduces B diffusion in SiO_2 and increases the viscosity.

1. Introduction

Silicon dioxide (SiO_2) is one of the most important materials in silicon (Si) devices, especially for a gate insulator film of metal-oxide-semiconductor (MOS) transistors. With the scaling down of MOS transistors, an ultrathin SiO_2 layer is demanded for the gate insulator. As the thickness of the SiO_2 layer decreases, atomic and molecular diffusion in SiO_2 becomes a fundamental issue. The diffusion in SiO_2 is also an important issue in high-k gate dielectrics because an interfacial SiO_2 layer forms between high-k gate films and Si substrates during postannealing.[1] In addition, boron (B) penetration from the gate electrode through the thin SiO_2 layer into the Si substrate has been recognized as a serious problem.[2] It is well known that the incorporation of N into SiO_2, or using Si oxynitride for the gate insulator, retards the B penetration.[3] Therefore, N atoms are also incorporated into the interfacial SiO_2 layer between high-k gate films and Si substrates.[4] However, the mechanism for the retardation of B diffusion in SiO_2 by the existence of N is not yet clear. Moreover, the diffusion in SiO_2 is closely related to the viscosity of SiO_2, which is an important property of materials. The viscous flow of SiO_2 reduces the oxidation-induced strain, which is caused by a 125% volume expansion, and therefore, plays an important role in thermal oxidation.[5]

The present work investigates the mechanism of Si self-diffusion and B diffusion in SiO_2, and the effect of N on the diffusion. The authors observe Si self-diffusion and B diffusion in $^{28}SiO_2$ samples implanted with ^{30}Si and B, and, based on the simulation, show that SiO is the diffusing species that mainly governs the diffusion in SiO_2. In addition, the enhancement of SiO diffusion by the existence of high-concentration B is described. Moreover, the authors investigate the effect of N on SiO diffusion based on the simulation of the thickness in Si thermal oxynitridation, where it is shown that SiO diffusion in SiO_2 is retarded by the incorporation of N.

2. Si Self-Diffusion

An isotopically enriched ^{28}Si single-crystal epilayer was thermally oxidized in dry O_2 at 1100 °C to form $^{28}SiO_2$ of thicknesses of 200, 300, and 650 nm. The samples were implanted with ^{30}Si at 50 keV to a dose of 2×10^{15} cm^{-2} and were capped with a 30 nm thick Si nitride layer by radio frequency (rf) magnetron sputtering. The as-implanted ^{30}Si profile is seen in the figures shown later in this article. Samples were annealed at temperatures between 1100 and 1250 °C. The depth profiles of ^{30}Si were measured by secondary ion mass spectrometry (SIMS). Figure 1 shows the experimental ^{30}Si depth profiles before and after annealing for 24 h at 1250 °C. The profiles demonstrate a strong dependence on the thickness of the $^{28}SiO_2$ layer; the thinner the $^{28}SiO_2$ layer, the broader the diffusion profile becomes.[6,7] This result shows that the Si self-diffusivity increases with decreasing the distance between the diffusing ^{30}Si species and the ^{28}Si-$^{28}SiO_2$ interface. This tendency was observed consistently in Si self-diffusion for the other temperatures and annealing times used in this study.

As the possible origins of the distance dependence of Si self-diffusion, the authors examined the effect of implantation damage; however, it is of no concern because the self-diffusivity of implanted Si in thick SiO_2 agrees with that obtained from damage-free chemical vapor deposition (CVD) SiO_2,[8,9] and remains unchanged for the doses be-

This article is a revised version of the paper printed in the *Proceedings of the First International Conference on Diffusion in Solids and Liquids—DSL-2005*, Aveiro, Portugal, July 6-8, 2005, Andreas Öchsner, José Grácio and Frédéric Barlat, eds., University of Aveiro, 2005.

Masashi Uematsu, NTT Basic Research Laboratories, NTT Corporation, 3-1 Morinosato Wakamiya, Atsugi 243-0198, Japan. Contact e-mail: uematsu@aecl.ntt.co.jp.

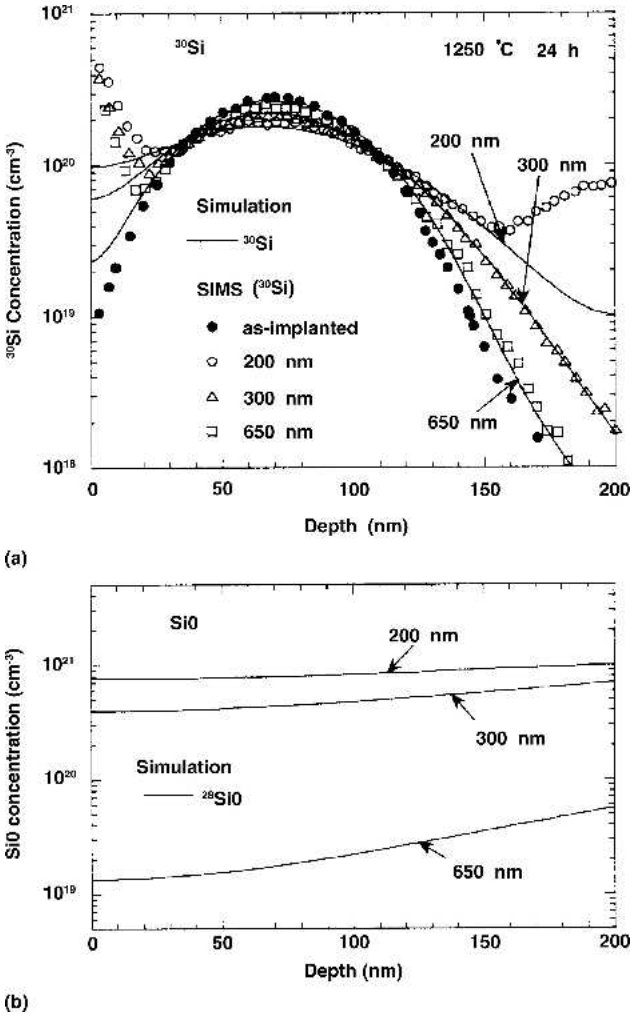

Fig. 1 Experimental and simulated (a) ^{30}Si depth profiles and (b) simulated SiO profiles in SiO_2 samples with various thicknesses. Samples were annealed at 1250 °C for 24 h. The as-implanted ^{30}Si profile is shown as the initial profile. In the SIMS data, the increase of ^{30}Si concentration deep in the bulk (>150 nm) in the 200 nm thick sample is ^{30}Si that diffused from ^{nat}Si substrates (800 nm below the ^{28}Si epilayer) during the thermal oxidation to prepare the sample. (^{nat}Si refers to Si with the natural isotopic abundance.)

tween 1×10^{14} and 2×10^{15} cm^{-2}. There was an evaluation of the stress due to an Si-nitride capping layer; however, its effect is too small to induce the large enhancement of the Si self-diffusion (a factor of 10 enhancement for the diffusion between 200 and 650 nm from the interface). Moreover, the authors performed an experiment using CVD isotope heterostructures with a constant total oxide thickness, and Si self-diffusivity increases with decreasing the distance from the interface in the same way as that described above.[10] These results lead us to conclude that Si species generated at the Si-SiO_2 interface and diffusing into SiO_2 enhance Si self-diffusion. There have been a number of suggestions, based on experimental speculations and theoretical predictions,[11,12] regarding the emission of Si species from the Si-SiO_2 interface to SiO_2, and SiO generated at the Si-SiO_2 interface via the reaction $Si + SiO_2 \rightarrow 2SiO$ is the most likely candidate as the dominant Si species. Consequently, the authors have proposed a model that SiO molecules, which are generated at the Si-SiO_2 interface and diffuse into SiO_2, enhance Si self-diffusion in SiO_2 via the reaction such that:

$$^{30}Si(s) + {}^{28}SiO \leftrightarrow {}^{28}Si(s) + {}^{30}SiO \quad \text{(Eq 1)}$$

$$^{30}Si(s) + {}^{28}Si(s) \leftrightarrow {}^{28}Si(s) + {}^{30}Si(s). \quad \text{(Eq 2)}$$

In these equations, Si atoms substituted in the Si sites of SiO_2 (denoted as *s*) diffuse via the kickout reaction with diffusing SiO molecules. In addition, a simple mechanism of Si self-diffusion via Si interstitials or vacancies is taken into account for the thermal Si self-diffusion. This mechanism is described by Eq 2, where SiO molecules are not involved in the diffusion. The evidence for the existence of two mechanisms (with and without SiO) is that very few SiO molecules arrive from the interface in the 650 nm thick sample, as will be shown later by the simulation.

The above model leads to the following set of coupled partial differential equations to describe the diffusion of ^{30}Si in $^{28}SiO_2$:

$$\frac{\partial C_{30_{Si}}}{\partial t} = \frac{\partial}{\partial x}\left(D_{Si}^{SD(th)} \frac{\partial C_{30_{Si}}}{\partial x} \right) - R \quad \text{(Eq 3)}$$

$$\frac{\partial C_{30_{SiO}}}{\partial t} = \frac{\partial}{\partial x}\left(D_{SiO} \frac{\partial C_{30_{SiO}}}{\partial x} \right) + R \quad \text{(Eq 4)}$$

$$\frac{\partial C_{28_{SiO}}}{\partial t} = \frac{\partial}{\partial x}\left(D_{SiO} \frac{\partial C_{28_{SiO}}}{\partial x} \right) - R \quad \text{(Eq 5)}$$

where *R* is the reaction term for Eq 1 given by:

$$R = k_f C_{30_{Si}} C_{28_{SiO}} - k_b C_{30_{SiO}} \quad \text{(Eq 6)}$$

The Si self-diffusivity is, as a whole, described by:

$$D_{Si}^{SD} = D_{Si}^{SD(th)} + D_{SiO}^{SD} \frac{C_{28_{SiO}}(x,t)}{C_{SiO}^{max}} \quad \text{(Eq 7)}$$

In these equations, C_x is the concentration of the corresponding species in Eq 1 and 2, $D_{Si}^{SD(th)}$ is the thermal Si self-diffusivity, D_{SiO} is the diffusivity of SiO, and k_f and k_b are the forward and backward rate constants of Eq 1, respectively. In Eq 7, $D_{SiO}^{SD} = D_{SiO} C_{SiO}^{max}/N_0$ is the Si self-diffusivity via SiO, where N_0 denotes the number of SiO_2 molecules in a unit volume of Si oxide. Here, C_{SiO}^{max} denotes the maximum SiO concentration in SiO_2 and is described as $C_{SiO}^{max} = 3.6 \times 10^{24} \exp(-1.07 \text{ eV/kT})$ cm^{-3}.[7] In Eq 3, the thermal Si self-diffusion (Eq 2) is represented by the diffusion term with $D_{Si}^{SD(th)}$, and $D_{Si}^{SD(th)} = 0.8 \exp(-5.2 \text{ eV/kT})$ cm^2/s,[8] which was experimentally obtained, is used for the simulation. In Eq 7, $C_{28_{SiO}}(x,t)$ depends on the depth and annealing times, which will be described below. The boundary condition for ^{28}SiO at the ^{28}Si-$^{28}SiO_2$ interface is given by $C_{28_{SiO(x=interface)}} = C_{SiO}^{max}$ to describe the generation of SiO at the interface. The amount of ^{30}SiO arriving at the ^{28}Si-$^{28}SiO_2$ interface is so small that the mixing of ^{28}Si with ^{30}Si at the interface is neglected. The boundary condition at the nitride-capped surface is represented by a zero-flux condition because the cappings act as barriers. Reactions 1 and 2 are assumed to

be so fast that the local equilibrium of the reaction is established, and hence the rate constants are set to be large enough. The parameters deduced from the simulation to fit the experimental profiles of ^{30}Si are D^{SD}_{SiO}, and $D^{SD}_{SiO} = 4 \times 10^4 \exp(-6.2\ eV/kT)\ cm^2/s$ was consistently obtained for all samples. The D^{SD}_{SiO} is comparable to the SiO diffusivities reported in Ref 12 and 13. Equations 3 to 5 were solved numerically by the partial differential equation solver ZOMBIE.[14]

Figure 1 shows the simulated ^{30}Si depth profiles after annealing for 24 h at 1250 °C together with the experimental profiles. For the simulated ^{30}Si profiles, the concentration of $^{30}Si(s)$ is shown because it is about two orders of magnitude larger than that of ^{30}SiO. The simulation results fit the experimental profiles of ^{30}Si for all $^{28}SiO_2$ thicknesses using the same parameter values. This is in contrast to the Si self-diffusivity obtained by a simple fitting, or under the assumption of a constant diffusion coefficient for each profile, which increases with decreasing $^{28}SiO_2$ thickness: 6×10^{-17}, 4×10^{-17}, and $1 \times 10^{-17}\ cm^2/s$ for 200, 300, 650 nm, respectively (the contribution from $D^{SD(th)}_{Si}$ at 1250 °C is $5 \times 10^{-18}\ cm^2/s$ for all thicknesses). For other temperatures, the simulation results also fit the ^{30}Si profiles for all $^{28}SiO_2$ thicknesses using the same parameter values for each temperature. In Fig. 1(b), the simulated SiO profiles are also shown (the concentration of ^{28}SiO is shown because it is a few orders of magnitude larger than that of ^{30}SiO). The SiO concentration in the ^{30}Si region increases with decreasing $^{28}SiO_2$ thickness. As expected from Eq 7, SiO with higher concentration leads to larger enhancement of ^{30}Si diffusion. Therefore, the ^{30}Si self-diffusivity, assuming a constant diffusion coefficient, increases with decreasing $^{28}SiO_2$ thickness. This thickness dependence arises because the SiO diffusion is so slow that the SiO concentration at the ^{30}Si region critically depends on the distance from the Si-SiO_2 interface, where the SiO is generated. In addition, the profile of SiO for the 650 nm thick sample shows that the SiO concentration is so small that Si self-diffusion cannot be explained only by the kickout diffusion via SiO (Eq 1). This is the evidence for the existence of the two mechanisms (with and without SiO), as described above.

The time dependence of Si self-diffusion also shows the validity of our model. Figure 2 shows the experimental and simulated ^{30}Si profiles and the simulated SiO profiles in the 300 nm thick sample for 6 and 30 h at 1250 °C. The Si self-diffusivities, assuming a constant diffusion coefficient, show an enhancement of factor of 4.5 and are $1 \times 10^{-17}\ cm^2/s$ for 6 h and $4.5 \times 10^{-17}\ cm^2/s$ for 30 h. From the simulation, it was found that the SiO concentration in the near-surface region becomes higher at longer annealing times until it reaches the maximum concentration. The time dependence arises because the SiO diffusion is so slow that more SiO molecules are arriving from the interface with time, and the self-diffusivity, assuming a constant diffusion coefficient, therefore increases for a longer annealing time. The simulated and experimental profiles almost coincide, and this confirms the validity of our model. In addition, this result eliminates the concerns related to the strain or damage because Si self-diffusion would decrease with time if the diffusion were affected by the strain or damage, which should be gradually relieved or reduced by the anneals.

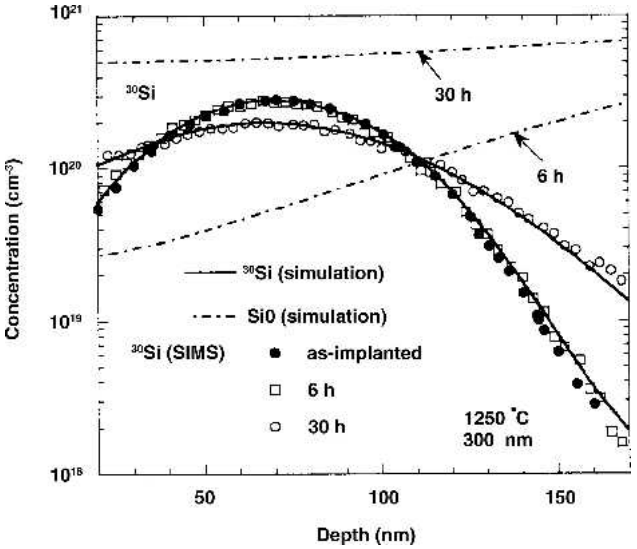

Fig. 2 Experimental and simulated ^{30}Si depth profiles and simulated SiO profiles in the 300 nm thick sample. Samples were annealed at 1250 °C for 6 and 30 h.

3. B Diffusion

The ^{30}Si-implanted samples mentioned in the previous section were subsequently implanted with ^{11}B at 25 keV to a dose of 5×10^{13} or $3 \times 10^{15}\ cm^{-2}$, which will be referred to as low-dose samples and high-dose samples, respectively. Samples were annealed, and the diffusion profiles of B and ^{30}Si were measured by SIMS. This simultaneous observation of B and ^{30}Si profiles allows us to investigate the effect of B concentration on diffusion, as decribed in the next section. Figure 3 shows the experimental B profiles in low-dose samples with various thicknesses after annealing at 1250 °C for 6 h. In the same way as Si self-diffusion, the B diffusion shows a clear dependence on the thickness of the $^{28}SiO_2$ layer; the shorter the distance from the Si-SiO_2 interface, the higher the B diffusivity in SiO_2.[15,16] This tendency was also observed for the high-dose samples and other temperatures used in this study. The distance dependence of B diffusivity indicates that the SiO molecules, which are generated at the Si-SiO_2 interface and diffusing into SiO_2, enhance not only Si self-diffusion but also B diffusion. In a similar manner to Si self-diffusion, B diffusion in SiO_2 is described by:

$$B(s) + {}^{28}SiO \leftrightarrow {}^{28}Si(s) + BO \qquad \text{(Eq 8)}$$

$$B(s) + Si(s) \leftrightarrow Si(s) + B(s) \qquad \text{(Eq 9)}$$

In Eq 8, B atoms substituted in the Si sites of SiO_2 diffuse via the kickout reaction with diffusing SiO. The B diffusion via SiO is similar to B diffusion in Si via the kickout mechanism, and BO may correspond to a complex of B-Si-O according to the first-principles calculation of B diffusion in SiO_2.[17] In addition, a simple mechanism of B diffusion, where SiO molecules are not involved, is taken into account

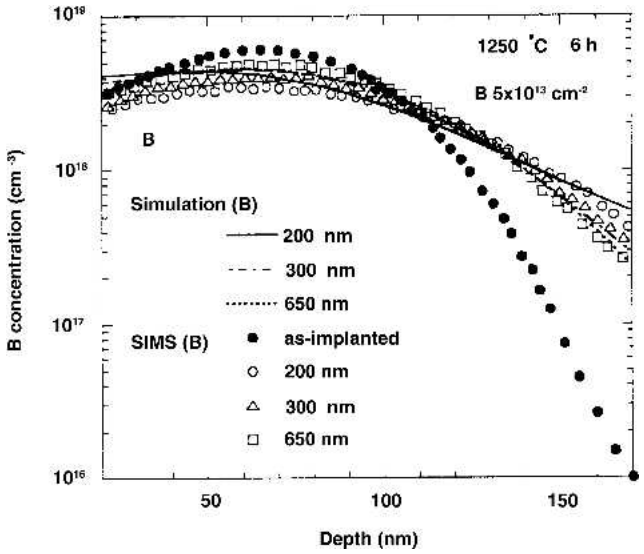

Fig. 3 Experimental and simulated B depth profiles in SiO_2 samples with various thicknesses. Samples were implanted with B to a dose of 5×10^{13} cm^{-2} (low B dose) and were annealed at 1250 °C for 6 h.

and is referred to as thermal B diffusion. Evidence for the existence of two mechanisms (with and without SiO) is that B diffusion occurs in the 650 nm thick sample, where very few SiO molecules arrive from the interface, as described above.

The B diffusion in SiO_2 is simulated in a manner similar to that of Si self-diffusion by replacing ^{30}Si with B in Eq 1 and 2. Likewise, $D_{Si}^{SD(th)}$ should be replaced with $D_B^{eff(th)}$ (the effective diffusivity of thermal B diffusion), and D_{SiO}^{SD} should be replaced with D_i^{eff} (the effective diffusivity of B diffusion via the kickout mechanism with SiO). The total effective B diffusivity is expressed by:

$$D_B^{eff} = D_B^{eff(th)} + D_i^{eff} \frac{C_{^{28}SiO}(x,t)}{C_{SiO}^{max}} \quad \text{(Eq 10)}$$

The experimentally obtained B diffusivity in thick (i.e., >1 μm) SiO_2, $D_B^{eff(th)} = 3.12 \times 10^{-3}$ exp(−3.93 eV/kT) cm^2/s,[18] which corresponds to the effective thermal B diffusivity, is used in our simulation. Consequently, the only parameter needed to fit the experimental B profiles in Fig. 3 is D_i^{eff}, and we consistently obtained $D_i^{eff} = 6.4 \times 10^{-2}$ exp(−4.1 eV/kT) cm^2/s for all samples.

Figure 3 shows the simulated B profiles after annealing for 6 h at 1250 °C. The simulation results fit the experimental B profiles for all the thicknesses using the same parameter values. This is in contrast to a simple fitting with a constant diffusivity, leading to 4×10^{-16}, 3×10^{-16}, and 2×10^{-16} cm^2/s for 200, 300, and 650 nm, respectively. For other temperatures, the simulation results also fit the B profiles for all $^{28}SiO_2$ thicknesses using the same parameter values for each temperature. In addition, the time-dependent B diffusion was also observed and simulated, in the same way as Si self-diffusion. These confirm the validity of our model that B diffusion in SiO_2 is enhanced by SiO. We mention that the effect of the Si-SiO_2 interface, which generates SiO molecules, should be taken into account for the analysis of diffusion in SiO_2. The D_{SiO} value deduced has the value of ~4×10^{-17} cm^2/s at 1100 °C, and the diffusion length for 10 s annealing is 2 $(D_{SiO} \times t)^{1/2} \sim 0.4$ nm. This estimation indicates that SiO from the interface may affect the phenomena in the bulk when the material thickness is down to 1 nm.

4. Effect of High-Concentration B

Figure 4 shows the depth profiles of ^{30}Si and B in the high-dose 200 nm thick sample after diffusion annealing of 6 h at 1250 °C. The ^{30}Si depth profile of the annealed sample without B implantation is also shown. The profile of ^{30}Si in the high-dose samples shows larger diffusion than that without B.[15,16] On the other hand, the ^{30}Si profile of the low-dose samples (not shown in Fig. 4) showed no significant difference from that without B. In addition, for the high-dose sample, a significant decrease in the ^{30}Si concentration at its peak region was observed, where B concentration is high. In contrast, the tail region of ^{30}Si showed less significant diffusion, where B concentration is low. These results show that Si self-diffusivity increases with higher B concentration in SiO_2.

This dependence of B concentration is also seen in B diffusion itself. Figure 4(b) compares the experimental and simulated B profiles in the 200 nm thick sample with high B dose after annealing at 1250 °C for 6 h. With the D_i^{eff} given above, the B diffusion profiles of low-dose samples were well-reproduced by the simulation, as described in the previous section. However, the same simulation of the B diffusion for high-dose samples underestimated the results, as shown by the dotted line. This result shows that B diffusion in high-dose samples is faster than that in low-dose samples and that B diffusivity also increases with higher B concentration. The B concentration dependence has been reported in an experiment using an MOS structure, where the B diffusivity abruptly increased above B concentration of 10^{20} cm^{-3},[19] which is consistent with our result.

To reproduce the experimentally obtained enhancement of the ^{30}Si and B diffusion in the high-dose sample, the authors introduced a B concentration dependence of D_{SiO}^{SD} and D_i^{eff} for Si self-diffusion and B diffusion via SiO, of $D_{Si}^{SD(th)}$ for thermal Si self-diffusion, and of $D_B^{eff(th)}$ for thermal B diffusion by multiplying a factor of $\exp(C_B/C_B^{cri})$ to imitate the strong dependence on B concentration, where C_B^{cri} denotes the critical B concentration above which the high-concentration effect occurs. The inclusion of the B concentration dependence ($\times\exp[C_B/C_B^{cri}]$) of $D_{Si}^{SD(th)}$ and $D_B^{eff(th)}$ is essential for explaining the enhancement of Si self-diffusion and B diffusion in the 650 nm thick sample, where very few SiO molecules arrive from the interface. Consequently, the factor $\exp(C_B/C_B^{cri})$ was applied to D_{Si}^{SD} (Eq 7) and D_B^{eff} (Eq 10), which represent the sum of the two contributions (thermal diffusion and diffusion via SiO) to Si self-diffusion and B diffusion (the value of C_{SiO}^{max} is not changed). Using the value of $C_B^{cri} = 2 \times 10^{20}$ cm^{-3}, ^{30}Si

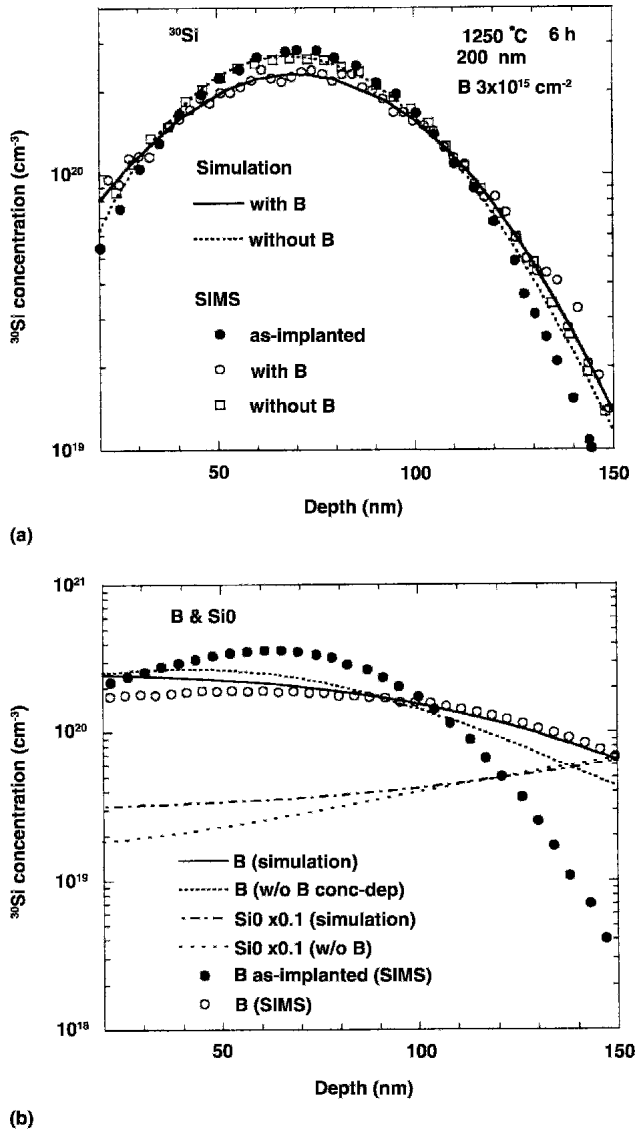

Fig. 4 (a) Experimental and simulated ^{30}Si depth profiles with high-dose B implantation (3×10^{15} cm^{-2}) and without B, and (b) experimental and simulated B depth profiles and the simulated SiO profile (multiplied by 0.1) with high B dose in the 200 nm thick sample after annealing for 6 h at 1250 °C. In (b), the result of simulation without B concentration dependence and the simulated SiO profile (multiplied by 0.1) without B are also shown.

and B profiles in the high-B-dose samples were fitted by the same set of diffusion parameters as that for low-dose profiles and that without B, as shown in Fig. 4. The profiles of SiO (multiplied by 0.1) obtained from the simulation are also shown in Fig. 4(b). In the near-surface region, the SiO concentration with high B dose is higher than that without B due to the enhanced SiO diffusivity by the B concentration dependence ($\times\exp[C_B/C_B^{cri}]$), which leads to the increase of Si self-diffusivity and B diffusivity with higher B concentration. The mechanism of this diffusion enhancement by high-concentration B will be discussed below. The present result indicates that Si and B atoms in SiO_2 diffuse correlatively via SiO; namely, the enhanced SiO diffusion by the existence of B enhances B diffusion and Si self-diffusion. This correlation is consistent with the theoretical result that SiO molecules diffuse predominantly with frequent atomic exchange interactions with substitutional atoms.[17]

5. Effect of N on Diffusion

In this section, the effect of N on diffusion in SiO_2 is investigated based on the knowledge obtained above and based on the simulation of Si oxynitridation. It is assumed that the incorporation of N reduces the SiO diffusivity in SiO_2 because the existence of N retards the B penetration, or B diffusion, which is enhanced by SiO. This assumption is also consistent with the increase of SiO_2 viscosity with N incorporation because the diffusion of SiO is closely related to the viscosity of SiO_2, and viscosity is inversely proportional to diffusivity.[20] To validate this assumption, the authors simulate the thickness of Si thermal N_2O oxynitridation based on our interfacial Si emission model, which has successfully simulated Si thermal oxidation.[21-24] In this model, a large number of SiO molecules (~1% of the oxidized Si) are emitted from the Si-SiO_2 interface during oxidation, and most of the emitted SiO molecules diffuse into the oxide. In addition, the oxidation becomes slower with higher SiO concentrations near the interface because the existence of high-concentration SiO prevents the emission of new SiO at the interface upon oxidation. Therefore, the oxidation in the oxide, which absorbs the emitted SiO, controls, or modulates, the oxidation rate at the interface. Based on the model, the authors constructed the diffusion equations of the SiO and oxidant with the reaction terms of the SiO oxidation and numerically solved the equations to simulate the oxide thickness.

What has been reported so far about N_2O oxynitridation can be summarized:

- The oxynitridation rate is much smaller than the O_2 oxidation rate and becomes smaller as oxynitride grows.[25-28]
- N_2O thermally decomposes via the reactions of $N_2O \rightarrow N_2 + O$ and $N_2O + O \rightarrow 2NO$, and the remaining atomic O rapidly recombines into O_2, resulting in N_2 (64.3%), O_2 (31.0%), and NO (4.7%) at 950 °C.[26] Therefore, most of the increase in the thickness occurs via O_2, and NO is the source of N via the reaction with Si at the interface.
- Most of the N atoms incorporated during the oxynitridation pile up at the Si-SiO_2 interface with a width of ~2 nm,[27] and the N concentration tends to saturate at only ~2 at.%.

Therefore, N_2O oxynitridation can be regarded as O_2 oxidation except that the piled-up N at the Si-SiO_2 interface affects the process. This leads to the application of the interfacial Si emission model to N_2O oxynitridation to simulate the thickness. In our model, therefore, SiO molecules are emitted from the Si-SiO_2 interface upon oxidation and diffuse in SiO_2 containing ~2 at.% N. The oxidation rate

constant k is reduced as the SiO concentration near the interface C^{I}_{SiO} increases as oxidation proceeds, because the existence of high-concentration SiO prevents the emission of new SiO at the interface. This reduction is described by:

$$k = k_0 \left(1 - \frac{C^{I}_{SiO}}{C^{max}_{SiO}} \right) \quad \text{(Eq 11)}$$

where k_0 is the maximum oxidation rate constant. Here, we assume that the incorporation of N into SiO_2 reduces the SiO diffusivity. The assumption that the SiO diffusivity exponentially decreases with increasing N concentration was introduced in analogy with B diffusivity in SiO_2, which exponentially increases with B concentration. During oxynitridation, the SiO diffusion is strongly retarded by the N at the interface. This retardation increases the SiO concentration in SiO_2 near the interface as oxynitridation proceeds, which decreases the oxynitridation rate with time.

For the simulation of N_2O oxynitridation, three parameters (i.e., C^{cri}_N, A_0, and C^{max}_N) are newly introduced into our interfacial Si emission model. The other parameter values are the same as those in our previous studies for thermal O_2 oxidation.[22,23] The dependence of the SiO diffusivity on N concentration, C_N, is described as:

$$D^{N}_{SiO} = D_{SiO} \exp\left(- \frac{C_N}{C^{cri}_N} \right) \quad \text{(Eq 12)}$$

where C^{cri}_N denotes the critical N concentration above which the N effect occurs. It is assumed that C^{max}_{SiO} is independent of the N concentration. The increase in N concentration with increasing thickness (x) was obtained by:

$$\Delta C_N = A \Delta x \quad \text{(Eq 13)}$$

for each calculation step. Here, A is the incorporation rate of N and is described by:

$$A = A_0 \left(1 - \frac{C_N}{C^{max}_N} \right) \quad \text{(Eq 14)}$$

which describes that the N concentration increases almost linearly with thickness in an early stage and then tends to saturate.[25] The C^{max}_N is the maximum N concentration. In the present simulation, all of the thicknesses can be simulated using $C^{max}_N = 2$ at.%. This value is consistent with the saturation of N concentration at ~2 at.%, which indicates that the N concentration dependence of A is reasonable. As mentioned above, most of the N atoms incorporated during the oxynitridation pile up at the Si-SiO_2 interface with a width of ~2 nm. In the simulation, the authors therefore set an N-containing SiO_2 layer with a width of 2 nm at the interface. The N concentration in this layer increases as oxynitridation proceeds.

The oxynitride thicknesses simulated in this study and obtained in other experiments[28] are shown in Fig. 5. In the simulation, the thickness increase results from the oxidation by O_2 produced from the thermal decomposition of N_2O, as

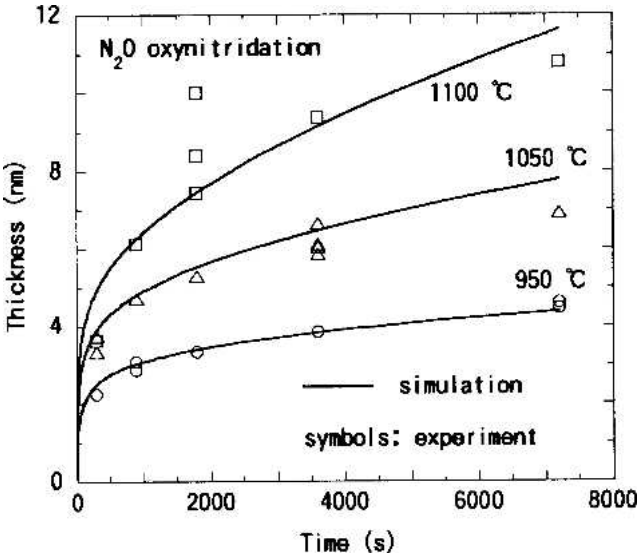

Fig. 5 Simulated and experimental oxynitride thickness. The experimental data are from Hussey et al.[28]

mentioned above. The proportion of O_2 is ~30%, and therefore the value of 0.3 atm was used as a partial pressure of O_2 in the simulation. Concerning the parameter values introduced for oxynitridation, $C^{max}_N = 2$ at.% was used, as previously mentioned. For C^{cri}_N, 0.16 at.% at 950 °C, 0.20 at.% at 1050 °C, and 0.23 at.% at 1100 °C were used to fit the thickness. The temperature dependence of C^{cri}_N is attributable to lower SiO_2 viscosity, or larger SiO diffusivity, at higher temperatures, which may reduce the effect of N. Concerning the value of A_0, it becomes smaller with smaller N_2O flow rate, and this is attributed to smaller N incorporation with slower flow.[26] Due to the lower N_2O flow rate, it takes longer for the NO to reach the substrates. With slower flow, therefore, the loss of NO by the reaction $2NO + O_2 \rightarrow 2NO_2$ is more likely to occur during the gas flow, resulting in smaller N incorporation. Therefore, the value of A_0 depends on the flow rate and, in addition, on the dimensions of the furnace used. In the present simulation, however, the thickness was consistently fitted using the same set of parameters when the oxynitride was grown under the same flow, as shown in Fig. 5, where $A_0 = 0.4$ at.%/nm was used to fit the thicknesses. Therefore, the simulation fits the experimental oxynitride thickness in a unified manner, and this indicates the validity of our assumption of the N effect on SiO diffusion.

The calculated depth profile of SiO deduced from the simulation for 1050 °C at 1000 s (Fig. 5) is shown in Fig. 6. The N atoms are incorporated into the layer with a width of 2 nm at the interface, as shown by the thick double-headed arrow. For the calculation, the interface is fixed at $x = 0$, while the surface moves as the oxynitridation proceeds. The oxynitride thickness is 5 nm, and the surface position is described by the vertical arrow (the right-hand side of the arrow is the gas phase). For comparison, Fig. 6 also shows the depth profile without N incorporation, that is, in pure O_2 oxidation, where the oxide thickness is 23 nm and the surface is outside the right ordinate. In oxynitridation, SiO

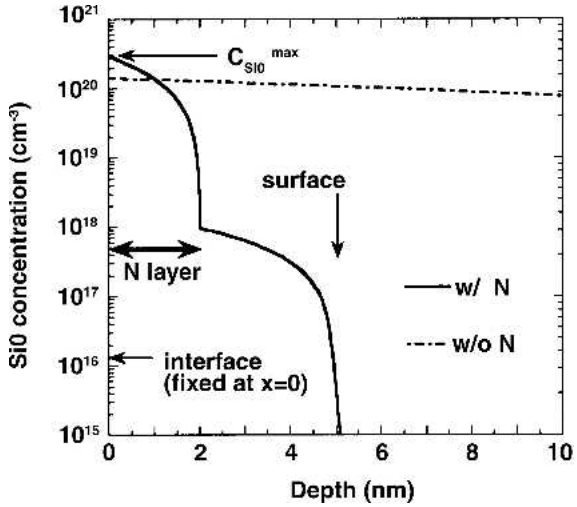

Fig. 6 Calculated depth profile of SiO deduced from the simulation conducted at 1050 °C for 1000 s in Fig. 5. For comparison, the calculated result without N incorporation is also shown. For the calculation, the interface is fixed at $x = 0$, while the surface moves as the oxynitridation proceeds. The surface position for oxynitridation is indicated by the vertical arrow. The N-containing layer with a width of 2 nm at the interface is also shown by the thick double-headed arrow.

diffusion is retarded at the N-containing layer, and the SiO concentration almost reaches C_{SiO}^{max} at this temperature. Therefore, the growth rate is significantly reduced (Eq 11). The concentrations of N incorporated after 2 h of the oxynitridation deduced from the simulation in Fig. 5 are 1.0, 1.5, and 1.8 at.% at 950, 1050, and 1100 °C, respectively. From Eq 12 and the C_N^{cri} values described above, the SiO diffusivity was found to decrease about three orders of magnitude. This result explains why B penetration, which is enhanced by SiO, is suppressed even with a small amount of N (~2 at.%).

As for the retardation of SiO diffusion by the existence of N, the formation of $Si_3 \equiv N$ bonds is a possible mechanism. SiO diffuses via the bond exchanges with Si and O atoms of SiO_2; that is, via the reconstruction of Si-O bonds, not via the interstitial mechanism through the open spaces of SiO_2. One N atom forms bonds with three Si atoms and can fix the SiO_2 framework as a brace, and, hence, N can effectively block the reconstruction of Si-O bonds in a wide area of the SiO_2 framework. Therefore, SiO diffusion in SiO_2 is significantly reduced even by a small amount of N. In contrast, the existence of B enhances SiO diffusion in SiO_2, as described in the previous section. The difference in the number of valence electrons between B (three) and Si (four) may be the origin of this enhancement. Due to the difference in the valence, substitutional B atoms will produce dangling bonds, which may ease the bond exchanges with Si and O atoms of SiO_2. Therefore, the introduction of B atoms leads to enhanced SiO diffusion in SiO_2. Because the diffusion of SiO is closely related to the viscosity of SiO_2, and because viscosity is inversely proportional to diffusivity, the present results indicate that the incorporation of B in SiO_2 reduces the viscosity of SiO_2, while that of N increases the viscosity, which is consistent with what has been known so far on the viscosity.

6. Conclusions

The authors have described the experimental and simulation results of Si self-diffusion and B diffusion in SiO_2, and have examined the effect of B and N on the diffusion. It is shown that SiO molecules enhance both Si self-diffusion and B diffusion in SiO_2. In addition, based on the B concentration dependence, the simulation result indicates that B and Si atoms in SiO_2 diffuse correlatively via SiO; namely, the enhanced SiO diffusion by the existence of B enhances both B diffusion and Si self-diffusion. In contrast, the incorporation of N in SiO_2 reduces the SiO diffusivity, which reduces B diffusion in SiO_2.

Acknowledgments

The research on diffusion in SiO_2 was a collaboration with Hiroyuki Kageshima (NTT), Yasuo Takahashi (Hokkaido University), Shigeto Fukatsu, Kohei M. Itoh (Keio University), Kenji Shiraishi (University of Tsukuba), and Ulrich Gösele (Max Planck Institute, Halle).

References

1. G.D. Wilk, R.M. Wallace, and J.M. Anthony, High-k Gate Dielectrics: Current Status and Materials Properties Considerations, *J. Appl. Phys.,* Vol 89, 2001, p 5243-5275
2. J.R. Pfiester, L.C. Parrillo, and F.K. Baker, A Physical Model for Boron Penetration Through Thin Gate Oxides from p^+ Polysilicon Gates, *IEEE Electron Device Lett.,* Vol 11, 1990, p 247-249
3. Z.J. Ma, J.C. Chen, Z.H. Liu, J.T. Krick, Y.T. Cheng, C. Hu, and P.K. Ko, Suppression of Boron Penetration in p^+ Polysilicon Gate p-MOSFET's Using Low-Temperature Gate-Oxide N_2O Anneal, *IEEE Electron Device Lett.,* Vol 15, 1994, p 109-111
4. Y. Morisaki, T. Aoyama, Y. Sugita, K. Irino, T. Sugii, and T. Nakamura, Ultra-Thin Poly-Si-Gate SiN/HfO_2/SiON High-k Stack Dielectrics with High Thermal Stability, *IEDM Tech. Dig.,* Int. Electron Devices Meeting Dec 8–11, 2002 (San Francisco, CA), p 861-864
5. M. Uematsu, H. Kageshima, and K. Shiraishi, Two-Dimensional Simulation of Pattern-Dependent Oxidation of Silicon Nanostructures on Silicon-on-Insulator Substrates, *Solid State Electron.,* Vol 48, 2004, p 1073-1078
6. S. Fukatsu, T. Takahashi, K.M. Itoh, M. Uematsu, A. Fujiwara, H. Kageshima, Y. Takahashi, K. Shiraishi, and U. Gösele, Effect of the Si/SiO_2 Interface on Self-Diffusion of Si in Semiconductor-Grade SiO_2, *Appl. Phys. Lett.,* Vol 83, 2003, p 3897-3899
7. M. Uematsu, H. Kageshima, Y. Takahashi, S. Fukatsu, K.M. Itoh, K. Shiraishi, and U. Gösele, Modeling of Si Self-Diffusion in SiO_2: Effect of the Si/SiO_2 Interface Including Time-Dependent Diffusivity, *Appl. Phys. Lett.,* Vol 84, 2004, p 876-878
8. T. Takahashi, S. Fukatsu, K.M. Itoh, M. Uematsu, A. Fujiwara, H. Kageshima, Y. Takahashi, and K. Shiraishi, Self-Diffusion of Si in Thermally Grown SiO_2 Under Equilibrium Conditions, *J. Appl. Phys.*, Vol 93, 2003, p 3674-3676

9. S. Fukatsu, T. Takahashi, K.M. Itoh, M. Uematsu, A. Fujiwara, H. Kageshima, Y. Takahashi, and K. Shiraishi, The Effect of Partial Pressure of Oxygen on Self-Diffusion of Si in SiO_2, Part 2, *Jpn. J. Appl. Phys.,* Vol 42, 2003, p L1492-L1494
10. S. Fukatsu, K.M. Itoh, M. Uematsu, H. Kageshima, Y. Takahashi, and K. Shiraishi, Effect of Si/SiO_2 Interface on Silicon and Boron Diffusion in Thermally Grown SiO_2, Part 1, *Jpn. J. Appl. Phys.,* Vol 43, 2004, p 7837-7842
11. T.Y. Tan and U. Gösele, Oxidation-Enhanced or Retarded Diffusion and the Growth or Shrinkage of Oxidation-Induced Stacking Faults in Silicon, *Appl. Phys. Lett.,* Vol 40, 1982, p 616-619
12. G.K. Celler and L.E. Trimble, Catalytic Effect of SiO on Thermomigration of Impurities in SiO_2, *Appl. Phys. Lett*., Vol 54, 1989, p 1427-1429
13. D. Tsoukalas, C. Tsamis, and J. Stoemenos, Investigation of Silicon Interstitial Reaction with Insulating Films Using the Silicon Wafer Bonding Technique, *Appl. Phys. Lett.,* Vol 63, 1993, p 3167-3169
14. W. Jüngling, P. Pichler, S. Selberherr, E. Guerrero, and H.W. Pötzel, Simulation of Critical IC Fabrication Processes Using Advanced Physical and Numerical Methods, *IEEE Trans. Electron Devices,* Vol ED-32, 1985, p 156-167
15. M. Uematsu, H. Kageshima, Y. Takahashi, S. Fukatsu, K.M. Itoh, and K. Shiraishi, Correlated Diffusion of Silicon and Boron in Thermally Grown SiO_2, *Appl. Phys. Lett.,* Vol 85, 2004, p 221-223
16. M. Uematsu, H. Kageshima, Y. Takahashi, S. Fukatsu, K.M. Itoh, and K. Shiraishi, Simulation of Correlated Diffusion of Si and B in Thermally Grown SiO_2, *J. Appl. Phys.,* Vol 96, 2004, p 5513-5519
17. M. Otani, K. Shiraishi, and A. Oshiyama, First-Principles Calculations of Boron-Related Defects in SiO_2, *Phys. Rev. B: Condens. Matter,* Vol 68, 2003, p 184112-1-8
18. T. Aoyama, H. Tashiro, and K. Suzuki, Diffusion of Boron, Phosphorus, Arsenic, and Antimony in Thermally Grown Silicon Dioxide, *J. Electrochem. Soc*., Vol 146, 1999, p 1879-1883
19. T. Aoyama, H. Arimoto, and K. Horiuchi, Boron Diffusion in SiO_2 Involving High-Concentration Effects, *Jpn. J. Appl. Phys.,* Vol 40, 2001, p 2685-2687
20. R.H. Doremus, Viscosity of Silica, *J. Appl. Phys.,* Vol 92, 2002, p 7619-7629
21. H. Kageshima, K. Shiraishi, and M. Uematsu, Universal Theory of Si Oxidation Rate and Importance of Interfacial Si Emission, Part 2, *Jpn. J. Appl. Phys.,* Vol 38, 1999, p L971-L974
22. M. Uematsu, H. Kageshima, and K. Shiraishi, Unified Simulation of Silicon Oxidation Based on the Interfacial Silicon Emission Model, Part 2, *Jpn. J. Appl. Phys.,* Vol 39, 2000, p L699-L702
23. M. Uematsu, H. Kageshima, and K. Shiraishi, Simulation of Wet Oxidation of Silicon Based on the Interfacial Silicon Emission Model and Comparison with Dry Oxidation, *J. Appl. Phys.,* Vol 89, 2001, p 1948-1953
24. H. Kageshima, M. Uematsu, K. Akagi, S. Tsuneyuki, T. Akiyama, and K. Shiraishi, Theoretical Study of Excess Si Emitted from Si-Oxide/Si Interfaces. Part 1, *Jpn. J. Appl. Phys.,* Vol 43, 2004, p 8223-8226
25. H.T. Tang, W.N. Lennard, M.Z. Allmang, I.V. Mitchell, L.C. Feldman, M.L. Green, and D. Brasen, Nitrogen Content of Oxynitride Films on Si(100), *Appl. Phys. Lett.,* Vol 64, 1994, p 3473-3475
26. P.J. Tobin, Y. Okada, S.A. Ajuria, V. Lakhotia, W.A. Feil, and R.I. Hedge, Furnace Formation of Silicon Oxynitride Thin Dielectrics in Nitrous Oxide (N_2O): The Role of Nitric Oxide (NO), *J. Appl. Phys.,* Vol 75, 1994, p 1811-1817
27. N.S. Saks, D.I. Ma, and W.B. Fowler, Nitrogen Depletion During Oxidation in N_2O, *Appl. Phys. Lett.,* Vol 67, 1995, p 374-376
28. R.J. Hussey, T.L. Hoffman, Y. Tao, and M.J. Graham, A Study of Nitrogen Incorporation During the Oxidation of Si(100) in N_2O at High Temperatures, *J. Electrochem. Soc.,* Vol 143, 1996, p 221-228